Structural Evolution of Subnano Platinum Clusters

AIHUA NIE,[1,2] JINPING WU,[1,3] CHENGGANG ZHOU,[1,3] SHUJUAN YAO,[1,2] CHEN LUO,[1,2] ROBERT C. FORREY,[4] HANSONG CHENG[1]

[1]*Institute of Theoretical Chemistry and Computational Materials Science, China University of Geosciences, Wuhan 430074, People's Republic of China*

[2]*Graduate school, China University of Geosciences, Wuhan 430074, People's Republic of China*

[3]*Faculty of Materials Science and Chemical Engineering, China University of Geosciences, Wuhan 430074, People's Republic of China*

[4]*Pennsylvania State University, Berks-Lehigh Valley College, Reading, Pennsylvania 19610-6009, USA*

Received 16 January 2006; accepted 21 February 2006
Published online 1 August 2006 in Wiley InterScience (www.interscience.wiley.com).
DOI 10.1002/qua.21011

ABSTRACT: We present a theoretical study of the structural evolution of small minimum energy platinum clusters, using density functional theory (DFT). Three growth pathways were identified. At the subnanoscale, clusters with triangular packing are energetically most favorable. At a cluster size of approximately $n = 19$, a structural transition from triangular clusters to icosahedral clusters occurs. A less energetically favorable transition from triangular clusters to fcc-like clusters takes place at around $n = 38$. Ionization potentials, electron affinities, and magnetic moments of the triangular clusters were also calculated. Understanding the structures and properties will facilitate studies of the chemical reactivity of Pt nanoclusters toward small molecules. © 2006 Wiley Periodicals, Inc. Int J Quantum Chem 107: 219–224, 2007

Key words: Pt clusters; structure evolution; structural transition; density functional theory

Introduction

A number of intense studies have been performed on clusters of precious and early transition metals at the nano/subnanoscales in recent years, largely because of their potential applications as building blocks for functional nanostructure materials, electronic devices, and nanocatalysts [1–10]. Platinum nanoparticles are of particular interest since they have been widely used in many heterogeneous catalytic processes [11]. To gain a detailed understanding of the catalytic properties of these nanoparticles, it is essential to understand the electronic structure of small platinum clusters. This is because clusters not only can serve as a tractable

Correspondence to: H. Cheng; e-mail: chengh@apci.com

Contract grant sponsors: Research Foundation for Outstanding Young Teachers (Grant No. CUGQNL0519), China University of Geosciences (Wuhan).

model for the nanoparticles but can also provide an excellent platform for systematic understanding of structure/property evolution as they grow from a small size to a large size and ultimately into the bulk. Because of their fundamental and technological importance, platinum clusters have been a subject of extensive theoretical and experimental studies [12–30]. Numerous clusters of various sizes were found to be thermodynamically stable or metastable. The purpose of the present study is not to reinvestigate the cluster structures that have been reported in literature. Instead, our main interest is to gain insight into the evolution of platinum cluster reactivity toward small molecules as the size of the clusters increases. This requires understanding of the evolution of cluster geometric structures as well as the evolution of cluster electronic structures. In doing so, we discovered several platinum cluster structures that have not been reported in the literature with more stable or comparable binding energies. These new structures can be important for a systematic understanding of cluster growth and physicochemical properties. The main results of our computational studies are presented in this work.

Computational Method

The present study used density functional theory (DFT) under the generalized gradients approximation (GGA) with the Perdew–Wang exchange-correlation functional (PW91) as implemented in DMol^3 package [31–35]. The spin-polarization scheme was employed to deal with the electronically open-shell system. A double numerical basis set augmented with polarization functions was used to describe the valence electrons with the core electrons described with effective core potential (ECP), which also accounts for the relativistic effect expected to be significant for heavy elements in the Periodic Table. Full electron calculations were also performed for selected clusters and the difference in the calculated cluster structures and the predicted relative stability between the ECP and full electron calculations was found to be very small. All cluster geometries were fully optimized without imposing symmetry constraints, except for the icosahedral structures for which point group symmetries were used to simplify the calculations. For each specific cluster size, an exhaustive search for minimum energy structures for the cluster was conducted and usually ended up with numerous stable isomers. The average cluster binding energy was calculated using the following equation:

$$\Delta E_n = [nE(\mathrm{Pt}) - E(\mathrm{Pt}_n)]/n, \quad (n = 2, 3, \ldots), \quad (1)$$

where E(Pt) represents the atomic energy of Pt, and $E(\mathrm{Pt}_n)$ is the energy of Pt_n cluster. Subsequently, we evaluated the cluster ionization potential (IP), electron affinity (EA) and magnetic moment (μ) defined by

$$\mathrm{IP}_n = E(\mathrm{Pt}_n^+) - E(\mathrm{Pt}_n), \quad (2a)$$

$$\mathrm{EA}_n = E(\mathrm{Pt}_n^-) - E(\mathrm{Pt}_n), \quad (2b)$$

$$\mu = (m_u - m_d)/2, \quad (2c)$$

where m_u and m_d are the numbers of spin–up and spin–down electrons with $m_u > m_d$, respectively.

The cluster structural search follows essentially the idea of genetic algorithm by adding a new atom on top of the preceding minimum energy cluster and then searching for energetically most stable site. To avoid missing the energetically more stable structures, additional caution was taken by placing the new addition to the preceding clusters with energies close to the minimum energy cluster followed by energy minimization. We found that starting with an unstable preceding structure usually resulted in an energetically less favorable cluster. An important guide for small Pt_n cluster structural search is to follow a compact triangular growth pattern, which often leads to a lower energy structure.

Results and Discussion

Like other metal clusters, there are numerous isomers for each given size of platinum clusters. Figure 1 depicts the lowest energy structures of platinum clusters, where the average binding energy is also labeled underneath the structure. By definition, Eq. (1), the lowest energy structure corresponds to the structure with the largest average binding energy. The white ball shown in cluster Pt_n denotes the new addition from the preceding cluster Pt_{n-1}. The cluster structures with n = 2–7,10 have been previously reported [12–23]. To our knowledge, the structures for n = 8, 9,11—15 shown in Figure 1 are reported for the first time. The structures shown in Figure 1 are of higher or comparable

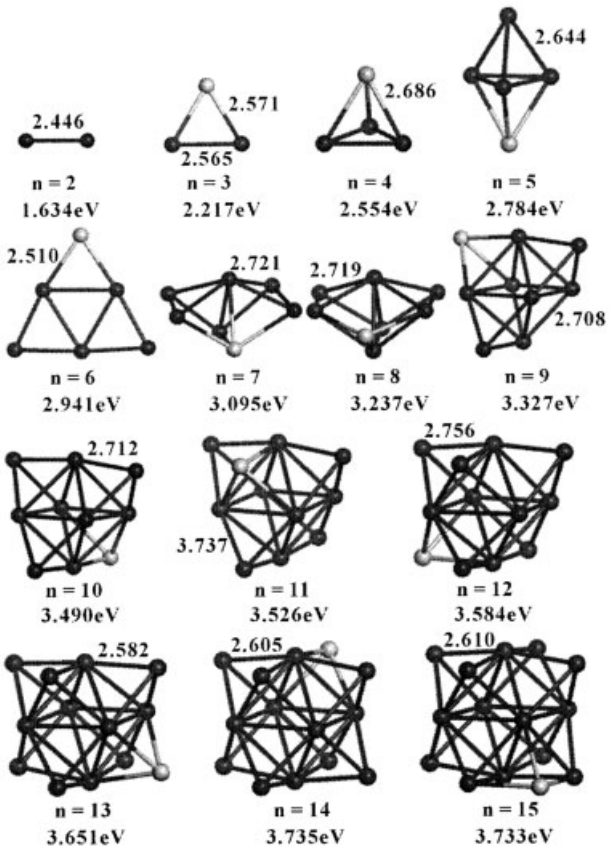

FIGURE 1. Lowest energy structures for Pt_n clusters (n = 2–15) and the calculated average binding energies per atom. The unit for the bond length is Ångstroms (Å).

binding energies compared with the previously reported structures. While the structures of n = 2, 3, and 6 are two-dimensional (2D), Pt_4 and Pt_5 adopt a 3D configuration with a tetrahedral geometry and a fused tetrahedral geometry, respectively. An abrupt structural change occurs from Pt_5 to Pt_6 with the triangular bipyramid geometry changed into a nearly equilateral triangle. In addition to the 2D equilateral triangular structure, we also obtained an octahedral structure for Pt_6 whose average binding energy, 2.886 eV, is only slightly smaller than that of the equilateral structure, which is 2.941 eV. It is possible that both geometries may exist for this cluster. It appears more natural for the clusters to grow three-dimensionally from Pt_4. Pt_7 can be viewed as two square pyramids fused with a triangular face from each. It is the basic structure on top of which small platinum clusters grow. By adding an atom on top of one of the fused edges, Pt_8 is formed. Placing a Pt atom on Pt_8 to form Pt_9 results in significant distortion. From Pt_{10}, the clusters grow successively on top of the preceding structure without significant structural deformation.

To compare with the structures of previously reported small Pt clusters, we chose Pt_8 and Pt_9 for further analysis. Figure 2 shows several isomers obtained from Ref. [23]. We further optimized these structures using the computational method employed in the present study. The calculated average binding energies are also shown in Figure 2. It was reported that the cubic structure was the most stable isomer of Pt_8 and capping an atom on the cubic structure yielded the most stable structure for Pt_9 [23]. The average binding energies calculated with our computational method for these two structures are 3.200 eV and 3.301 eV, respectively, considerably smaller than those of the lowest energy structures shown in Figure 1. In addition, the lowest energy structures are more closely packed with the average bond length of 2.683 Å for Pt_8 and 2.609 Å for Pt_9, respectively, compared with the average

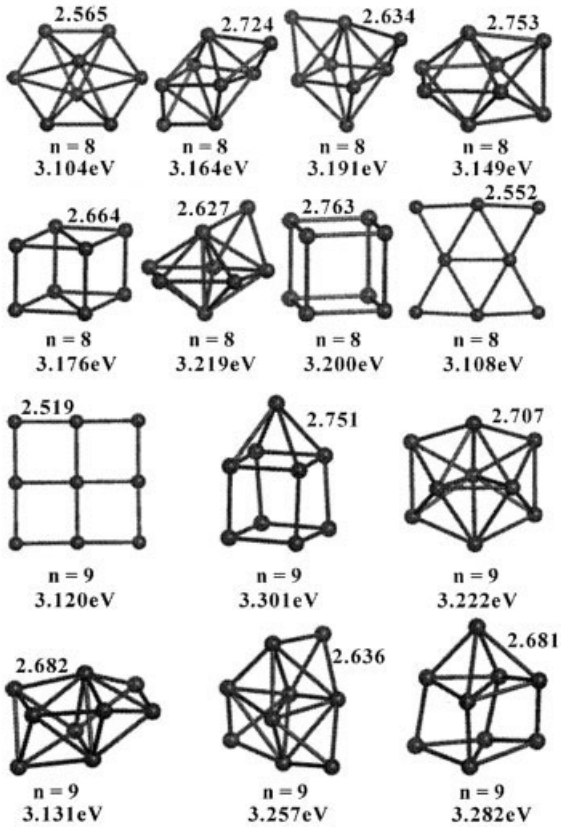

FIGURE 2. Selected isomers of Pt_8 and Pt_9 and the calculated average binding energies per atom. The unit for the bond length is Ångstroms (Å).

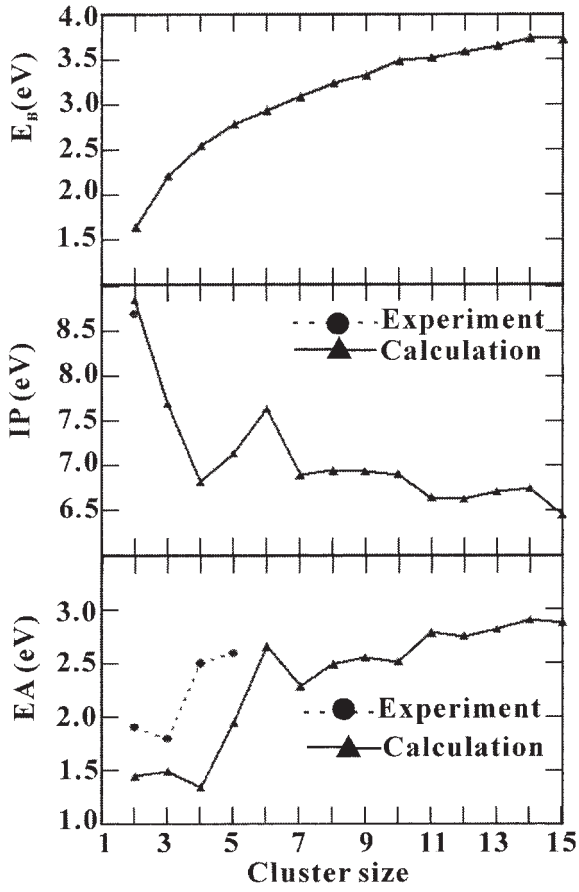

FIGURE 3. (a) Calculated binding energy per Pt atom (E_B) as a function of cluster size. (b) Ionization potential (IP). (c) Electron affinity (EA). The experimental values were taken from Refs. [27–30].

bond length of 2.763 Å for the cubic structure of Pt_8 and 2.683 Å for the capped cubic structure of Pt_9.

As the cluster size increases, the average binding energy of the clusters also increases [Fig. 3(a)], indicating that the clusters become increasingly stabilized. The calculated ionization potential (IP) and electron affinity (EA) are shown in Figure 3(b) and 3(c), respectively. Comparison with the available experimental data [27–30] suggests that the experimentally measured IP can be reproduced reasonably well. The calculated EAs deviate from the experimental values considerably, although the qualitative trend is consistent with the experimental results except Pt_4. It is possible that the structure of the anionic species Pt_4^- generated in the photoelectron spectroscopic experiments may differ from the tetrahedral geometry, although the computational results obtained in this study as well as in the studies by others [13, 17] suggest that the tetrahedral structure is the energetically most favorable geometric configuration. Indeed, besides the tetrahedral structure of Pt_4, which we found no appreciable structural change upon electron attachment to the fully optimized neutral cluster, we also obtained other geometric configurations such as square, rectangle, and rhombus. Although none of these structures is as stable as the tetrahedral geometry, the calculated EAs are much closer to the experimental value with the square geometry of 2.15 eV, rectangle of 2.66 eV, and rhombus of 2.46 eV. The reported experimental value is 2.5 ± 0.1 eV [30]. Furthermore, we attribute the underestimation of the cluster EAs shown in Figure 3(c) mainly to the fact that the present computational method does not include diffusion functions in the basis set, which is known to be essential for accurate electronic structure calculations of anionic species. The calculations indicate that the IP of small Pt clusters generally decreases with the cluster size and thus becomes easier to oxidize, while the EA increases with the cluster size with relatively a small variation for larger clusters. With an electronic configuration of $5d^9 6s^1$ for the Pt atom, Pt clusters may possess unpaired electrons and thus can be intrinsically magnetic. Figure 4 displays the calculated total magnetic moments of the clusters, where comparison with the results of a previous DFT study [23] was made. Our results indicate that the magnetic moment of the clusters are generally smaller than 2, while Ref. [23] reported a larger magnetic

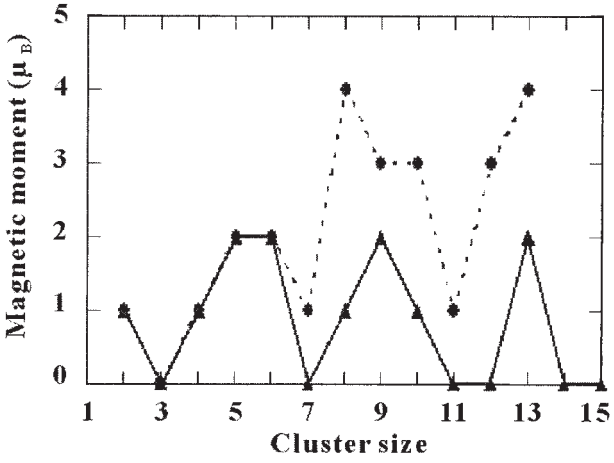

FIGURE 4. Calculated magnetic moment (μ) of Pt clusters as a function of cluster size. Data taken from Ref. [23] are denoted by solid dots; the values obtained from the present study are shown as solid triangles.

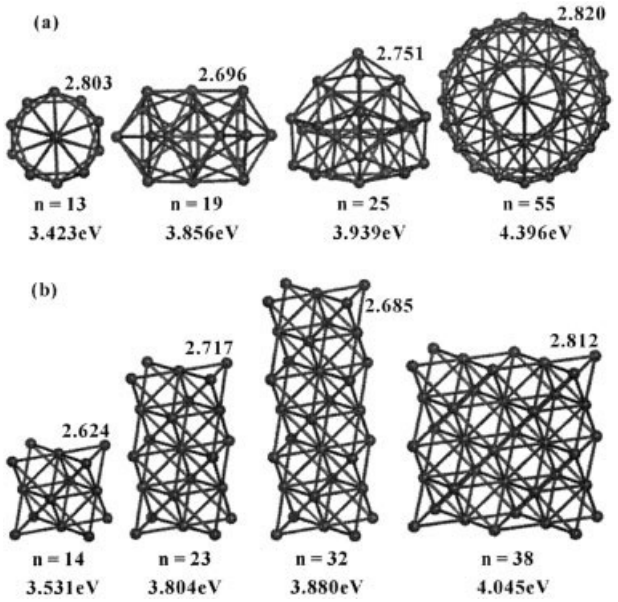

FIGURE 5. Optimized Pt clusters adopting an icosahedral growth pattern (a) and a fcc-like growth pattern (b). The unit for the bond length is Ångstroms (Å).

moment for clusters larger than $n = 7$. The discrepancy in the calculated magnetic moments arises from the fact that the present calculations yielded different but energetically more stable Pt clusters. We also note that the 5*d* and 6*s* orbitals of Pt atom are nearly degenerated and thus a change from a high spin state to a lower spin state (and vice versa) in the cluster should not give rise to a significant energy penalty.

To gain further insight into the growth of larger clusters, we selected 4 clusters adopting an icosahedral symmetry (n = 13, 19, 25, and 55) and 4 clusters with fcc-like geometry to examine the structural evolution. The optimized structures are shown in Figure 5, where the main geometric parameters are also labeled. In addition, we used the same computational method to compute the bulk structure and binding energy by imposing a periodic boundary condition. The calculated bond distance is within 0.087 Å difference from the experimental value and the calculated binding energy is 5.40 eV, in good agreement with the experimental value of 5.77 eV [36, 37].

Figure 6 displays the calculated binding energies of the triangular, icosahedral, and fcc-like clusters

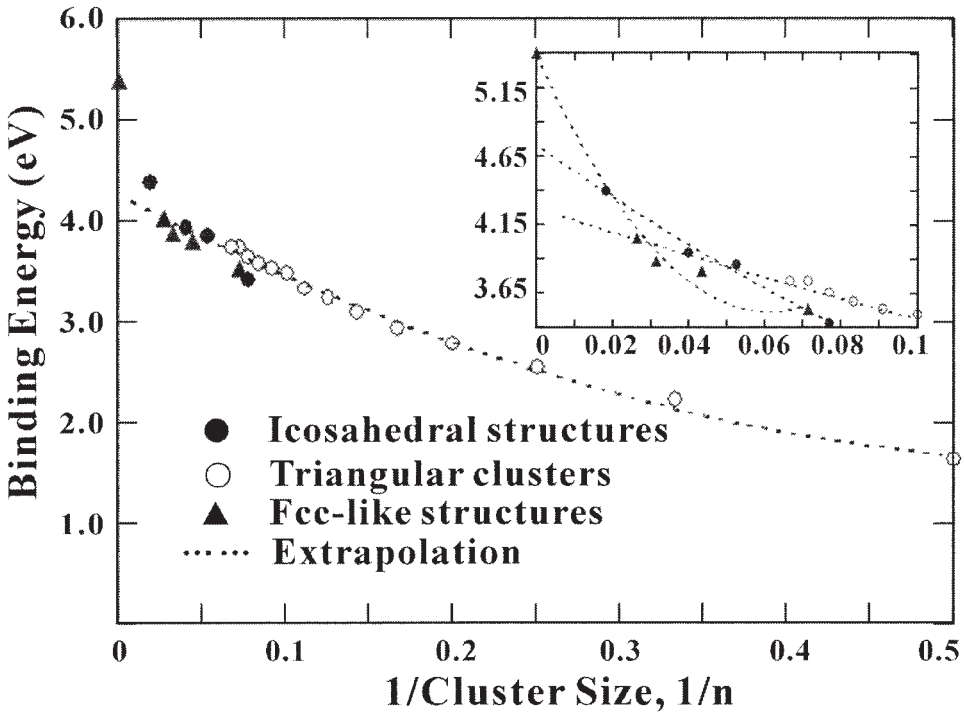

FIGURE 6. Comparison of binding energies between the lowest energy clusters and the clusters adopting the fcc growth pathway.

vs. the inverse of the cluster size. By interpolating/extrapolating the binding energy curves, we found that at about $n = 19$, an abrupt structural transition from the triangular clusters to the icosahedral clusters will occur. It can also be identified that a structural transition from the triangular clusters to the fcc-like clusters can occur at approximately $n = 38$, although the transition is less likely to happen because small fcc-like clusters are energetically less favorable than the icosahedral clusters. Unfortunately, it is difficult to identify the structural transition from the icosahedral clusters to the fcc-like clusters because too few points are available for data interpolation/extrapolation.

Summary

We have performed extensive computational studies of the minimum energy structure, properties, and growth of small Pt clusters based on DFT. We attempted to address the critical issue of Pt cluster evolution from subnano/nano size to bulk by examining three different growth pathways and by identifying the approximate sizes where structural transition between different growth pathways takes place. At the subnanoscale, the clusters essentially adopt a triangular growth pattern. Subsequently, at approximately $n = 19$, an abrupt transition to the icosahedral structures occurs. Based on the limited calculated data, it is envisaged that the structural transition from icosahedral clusters to the fcc-like clusters will occur at a very large number. We have also calculated some of the physical properties of the small triangular clusters and found that the magnetic moment of a cluster is size- and structure-dependent. A minimum energy cluster tends to have a smaller magnetic moment due to stronger electron pairing. The present study of small minimum energy Pt clusters allows us to conduct further studies of the chemical reactivity of Pt nanocluster toward small molecules, which will be published in due course.

References

1. Cheng, H.; Wang, L. S. Phys Rev Lett 1996, 77, 51.
2. Wang, L. S.; Wu, H.; Cheng, H. Phys Rev B 1997, 55, 884.
3. Pappas, D. P.; Popov, A. P.; Anisimov, A. N.; Reddy, B. V.; Khanna, S. N. Phys Rev Lett 1996, 76, 4332.
4. Lee, K.; Callaway, J.; Dhar, S. Phys Rev B 1984, 30, 1724.
5. Lee, K.; Callaway, J.; Dhar, S. Phys Rev B 1985, 31, 1796.
6. Castro, M.; Salahub, D. R. Phys Rev B 1994, 49, 11842.
7. Mirkin, C. A.; Letsinger, R. L.; Mucic, R. C.; Storhoff, J. J. Nature 1996, 382, 607.
8. Hong, B. H.; Bae, S. C.; Lee, C. W.; Jeong, S.; Kim, K. S. Science 2001, 294, 348.
9. Haruta, M. Catal Today 1997, 36, 153.
10. Häkkinen, H.; Abbet, S.; Sanchez, A.; Heiz, U. Angew Landman Chem Int Ed 2003, 42, 1297.
11. Van Santen, R. A. World Scientific Lecture and Course Notes in Chemistry; Vol. 5; World Scientific: Singapore, 1991.
12. Balasubramanian, K. J Chem Phys 1987, 84, 6573.
13. Dai, D.; Balasubramanian, K. J Chem Phys 1995, 103, 648.
14. Majumdar, D.; Dai, D.; Balasubramanian, K. J Chem Phys 2000, 113, 7919.
15. Majumdar, D.; Dai, D.; Balasubramanian, K. J Chem Phys 2000, 113, 7928.
16. Yang, S. H.; Drabold, D. A.; Adams, J. B.; Ordejon, P.; Glassford, K. J Phys Condens Matter 1997, 9, L39.
17. Fortunelli, A. J. Mol Struct 1999, 493, 233.
18. Varga, S.; Fricke, B.; Nakamatsu, H.; Mukoyama, T.; Anton, J.; Geschke, D.; Heitmann, A.; Engel, E.; Basütug, T. J Chem Phys 2000, 112, 3499.
19. Cui, Q.; Musaev, D. G.; Morokuma, K. J Chem Phys 1998, 108, 8418.
20. Grönbeck, H.; Andreoni, W. Chem Phys 2000, 262, 1.
21. Li, T.; Balbuena, P. B. J Phys Chem B 2001, 105, 9943.
22. Tian, W.-Q.; Ge, M.; Sahu, B. R.; Wang, D.; Yamada, T.; Mashiko, S. J Phys Chem A 2004, 108, 3806.
23. Xiao, L.; Wang, L. J Phys Chem A 2004, 108, 8605.
24. Apra, E.; Fortunelli, A. J Phys Chem A 2003, 107, 2934.
25. Apra, E.; Fortunelli, A. J Mol Struct 2000, 501/502, 251.
26. Watari, N.; Ohnishi, S. Phys Rev B 1998, 58, 1665.
27. Taylor, S.; Lemire, G. W.; Hamrick, Y. M.; Fu, Z.; Morse, M. D. J Chem Phys 1988, 89, 5517.
28. Ho, J.; Polak, M. L.; Ervin, K. M.; Lineberger, W. C. J Chem Phys 1993, 99, 8542.
29. Ervin, K. M.; Ho, J.; Lineberger, W. C. J Chem Phys 1988, 89, 4514.
30. Pontius, N.; Bechthold, P. S.; Neeb, M.; Eberhardt, W. J Electron Spectrosc Relat Phenom 2000, 106, 107.
31. Perdew, J. P.; Wang, Y. Phys Rev B 1992, 45, 13 244.
32. Delley, B. J Chem Phys 1990, 92, 508.
33. Delley, B. J Phys Chem 1996, 100, 6107.
34. Delley, B. Int J Quantum Chem 1998, 69, 423.
35. Delley, B. J Chem Phys 113, 2000, 7756.
36. Kittel, C. Introduction to Solid State Physics; 7th ed.; John Wiley & Sons: New York, 1996.
37. Voter, A. F. Los Alamos Unclassified Technical Report LA-UR 93-3901, 1993.